Research Paper

Inhibition of platelet function using liposomal nanoparticles blocks tumor metastasis

Yinlong Zhang[1,2], Jingyan Wei[1✉], Shaoli Liu[1,2], Jing Wang[2], Xuexiang Han[2], Hao Qin[2,4], Jiayan Lang[2], Keman Cheng[2,3], Yiye Li[2], Yingqiu Qi[2], Greg J Anderson[5], Saraswati Sukumar[6], Suping Li[2✉], Guangjun Nie[2,4✉]

1. College of Pharmaceutical Science, Jilin University, Changchun 130021, China;
2. CAS Key Laboratory for Biomedical Effects of Nanomaterials & Nanosafety, CAS Center for Excellence in Nanoscience, National Center for Nanoscience and Technology, Beijing 100190, China;
3. Department of Biomaterials, College of Materials, Xiamen University, Xiamen, 361005, China;
4. University of Chinese Academy of Sciences, Beijing 100049, China.
5. QIMR Berghofer Medical Research Institute, Royal Brisbane Hospital, QLD 4029, Australia.
6. Department of Oncology, Johns Hopkins University School of Medicine, Baltimore, MD21231, USA.

✉ Corresponding authors: Guangjun Nie, Ph.D, National Center for Nanoscience and Technology (NCNST), China Email: niegj@nanoctr.cn; Jingyan Wei, Ph.D, College of Pharmaceutical Science, Jilin University, Changchun, China Email: jingyanweijluedu@163.com; Suping Li, Ph.D, National Center for Nanoscience and Technology (NCNST), China Email: lisuping@nanoctr.cn.

Abstract

Extensive evidence has shown that platelets support tumor metastatic progression by inducing epithelial-mesenchymal transition of cancer cells and by shielding circulating tumor cells from immune-mediated elimination. Therefore, blocking platelet function represents a potential new avenue for therapy focused on eliminating metastasis. Here we show that liposomal nanoparticles bearing the tumor-homing pentapeptide CREKA (Cys-Arg-Glu-Lys-Ala) can deliver a platelet inhibitor, ticagrelor, into tumor tissues to specifically inhibit tumor-associated platelets. The drug-loaded nanoparticles (CREKA-Lipo-T) efficiently blocked the platelet-induced acquisition of an invasive phenotype by tumor cells and inhibited platelet-tumor cell interaction *in vitro*. Intravenously administered CREKA-Lipo-T effectively targeted tumors within 24 h, and inhibited tumor metastasis without overt side effects. Thus, the CREKA-Lipo formulation provides a simple strategy for the efficient delivery of anti-metastatic drugs and shows considerable promise as a platform for novel cancer therapeutics.

Key words: Tumor associated platelets, tumor metastasis, liposomal nanoparticle, metastatic inhibition.

Introduction

Metastasis is responsible for approximately 90% of human cancer deaths [1-2], so developing therapies to prevent tumor metastasis is of great importance in order to achieve long term cures.

Platelets have been shown to play a critical role in the development of tumor metastases. They can act in the primary tumor to stimulate tumor cells to acquire invasive properties, they have been shown to bind to circulating tumor cells to protect them as they travel to distant sites, and also to assist metastatic cells to become established at the distant sites [3-4]. In contrast to the heterogeneity displayed by tumor cells, platelets are relatively invariable; thus targeting them is potentially, promising method of inhibiting

metastasis. Numerous studies have shown that intratumoral platelets contain high levels of TGF-ß [5-6] and that the release of TGF-ß by platelets leads to acquisition of an invasive mesenchymal-like cell phenotype by the tumor cells [5]. Circulating platelets can also protect tumor cells from attack by natural killer (NK) cells either by shielding epitopes that NK cells recognize on the tumor cell surface, or by transferring major histocompatibility complex I (MHC I) proteins to the tumor cells [7-8]. In addition, tumor-associated platelets can release several permeability factors and enzymes that assist metastatic tumor cells to engraft at distant sites [9-10]. Since platelets play such an important role in the

metastatic process, repressing platelet functions represents a potential therapeutic approach to reducing metastasis. The few published studies targeting platelets to prevent cancer metastasis have either depleted circulating platelets or have used systemically administered drugs to inhibit platelet function [11-13]. Although effective in blocking tumor metastasis, severe bleeding is a major complication of these approaches, thereby limiting their clinical utility [14]. New strategies targeting platelet functions that have manageable or no bleeding or other side effects are urgently needed for anti-metastatic therapy.

Targeted nanomaterials have led to a revolution in drug delivery. Either passive or active targeting to sites of disease can lead to strong therapeutic efficacy with limited side effects [15-17]. In fact, various types of liposome nanoparticles, such as Doxil and Paclitaxel, are already in use in the cancer clinic as drug delivery systems [18]. In this study, we developed a biocompatible liposomal nanoparticle, Lipo-T, which is capable of carrying a reversible platelet inhibitor, ticagrelor. Ticagrelor, a nucleoside analog is a reversible antagonist of the P2Y12 receptor on platelets, and is an FDA approved drug used in the treatment of thrombotic events caused by platelet aggregation in acute coronary syndrome or myocardial infarction [19]. The nanoparticles were designed with a tumor-homing pentapeptide (CREKA) on their surface that targets the fibrin-fibronectin complexes within the microthrombi that are found on the walls of tumor blood vessels [20-21]. We show that drug-loaded liposomal nanoparticles (CREKA-Lipo-T) actively bind to tumor vessel microthrombi and locally release ticagrelor, resulting in inhibition of tumor-associated platelet functions. Blockage of TGF-β release from platelets in the tumor microenvironment is possibly one mechanism by which CREKA-Lipo-T impedes the initiation of tumor cell metastasis (Figure 1A). Intravenous administration of CREKA-Lipo-T significantly blocked outgrowth of lung metastasis efficiently in mice with subcutaneously implanted 4T1 tumors without overt side effects, and, of note, without the complication of bleeding. This simple strategy renders anti-platelet drugs an attractive alternative for the treatment of tumor metastases.

Results and Discussion

Preparation and characterization of CREKA-Lipo-T nanoparticles

To prepare liposome nanoparticles decorated with functional ligands, 1,2-distearoyl-sn-glycero-3-phosphoethanolamine-N-[maleimide(polyethylene glycol)-3400] (DSPE-PEG-MAL) was first conjugated with the tumor-homing pentapeptide CREKA (Cys-Arg-Glu-Lys-Ala) using the Michael addition reaction [20-21] between the thiol group of the cysteine in the peptide and the maleimide group of the hydrophilic PEG under anaerobic conditions (Figure 1B). The successful conjugation of DSPE-PEG and CREKA peptide was verified by MALDI-TOF-MS, which demonstrated that the molecular weight of DSPE-PEG increased from 3800 to 4402 as predicted (Figure S1).

CREKA coated ticagrelor-loaded liposome nanoparticles (CREKA-Lipo-T) were prepared using an improved thin-film dispersion method (Figure 1C). Ticagrelor was encapsulated by the liposomes during nanoparticle self-assembly. To optimize the drug loading capacity, different liposome/drug weight ratios were tested. When the ratio was 40:5, the nanoparticles had the highest drug encapsulation efficiency (~85%), with a uniform size distribution, and thus low dispersity (Table S1). Consequently, a 40:5 ratio was used in subsequent studies. The CREKA-Lipo-T nanoparticles possessed a typical liposomal membrane structure as revealed by transmission electron microscopy (TEM) [22-23] (Figure 2 A, C). Dynamic light scattering (DLS) analysis showed that CREKA-Lipo-T had an average hydrodynamic diameter of approximately 164 nm, which is larger than the diameter of empty nanoparticles (CREKA-Lipo; 139 nm) (Figure 2 B,D). As a result of the addition of ticagrelor, the average zeta potential of the particles decreased from -44 mV to -47 mV (Table 1) showing that drug loading had an effect on the net charge of the nanoparticles. CREKA-Lipo-T nanoparticles were stable and there was no significant change in size or surface zeta potential after incubation in PBS for up to 10 days at pH 7.4 (Table 1).

To evaluate drug release profiles of CREKA-Lipo-T, we investigated the accumulative drug release at both pH 6.8 and 7.4. As shown in Figure S2, CREKA-Lipo-T has a relatively fast drug release profile in pH 6.8 than in pH 7.4. There was about 30% and 40% accumulative drug release within 24 h and 48 h in pH 6.8 condition.

Table 1. Stability of liposome nanoparticles. Characteristics of the liposome nanoparticles were studied before and after 10 days of storage using dynamic light scattering detection (DLS).

Time (days)	Groups	Hydrodynamic diameter(nm)	Zeta potential (mV)	Dispersity
0	CREKA-Lipo	139.2±1.43	-44.0±1.43	0.188
0	CREKA-Lipo-T	164.2±4.62	-47.4±2.70	0.090
10	CREKA-Lipo	140.6±0.95	-44.1±0.74	0.169
10	CREKA-Lipo-T	165.1±2.81	-42.8±0.98	0.114
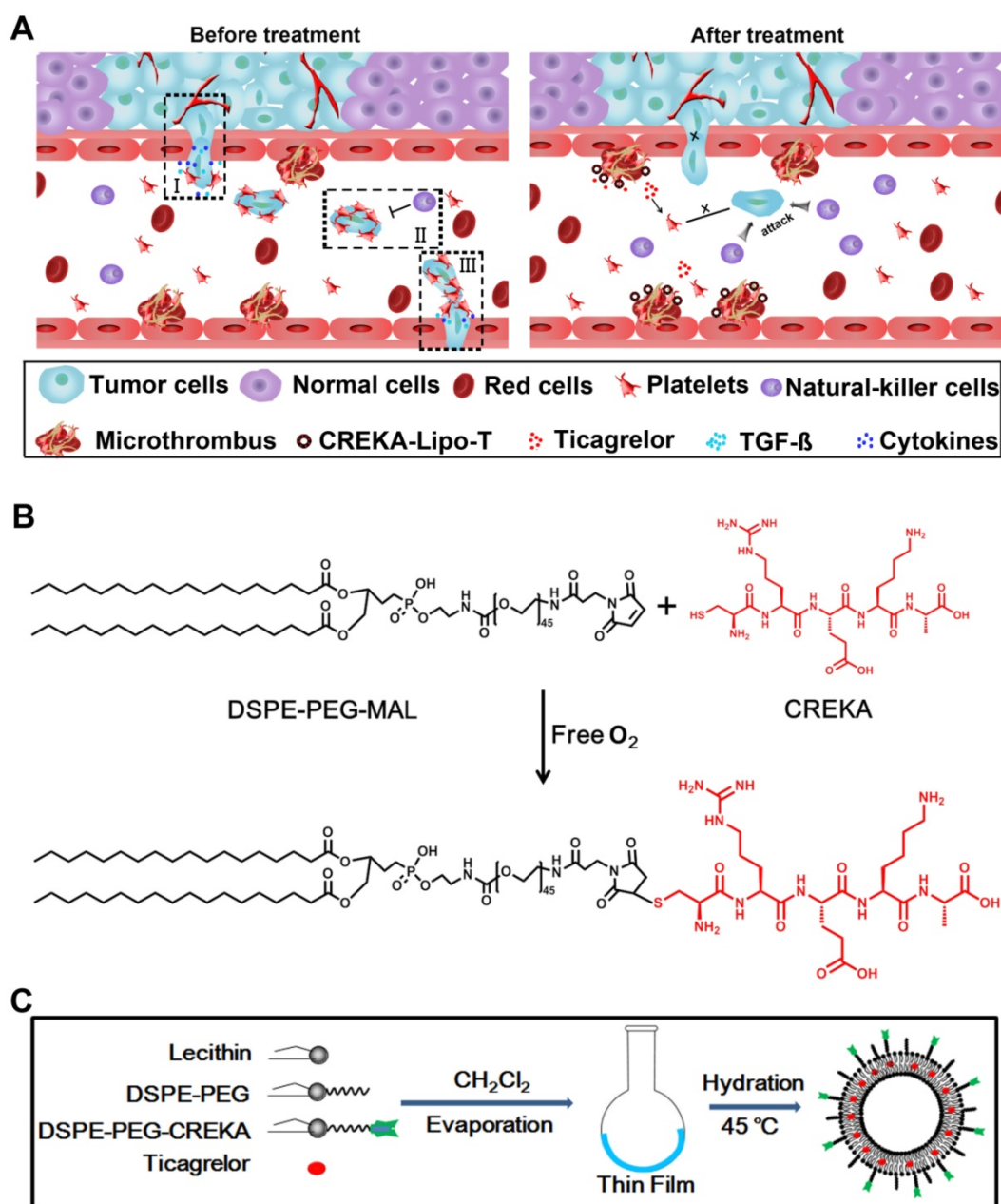
Figure 1. The design of CREKA-Lipo-T nanoparticles and their proposed anti-metastatic mechanism within tumor tissues. (**A**) Proposed mechanism of action of CREKA-Lipo-T nanoparticles. Normally, TGF-ß secreted by platelets induce the tumor cells to transition to a mesenchymal-like phenotype (I). Platelets can also protect tumor cells against attack from NK cells (II). At distant sites, platelets assist the metastatic cells to cross the local endothelium by secreting many cytokines. Following treatment, CREKA-Lipo-T actively targets to microthrombi on the tumor vessel walls and releases ticagrelor slowly and locally. Ticagrelor binds to tumor-associated platelets and inhibits their functions. The release of TGF-ß from platelets and the interaction between platelets and tumor cells are abolished, leading to decreased epithelial-mesenchymal-like transition of the tumor cells, and thus inhibiting their invasion capacity. When the tumor cells are present in the circulation, the compromised platelets are unable to adhere to them and cannot shield them from NK cell attack. X indicates that a process was abolished by treatment. (**B**) The conjugation between DSPE-PEG and the CREKA peptide using the Michael addition reaction under anaerobic conditions. (**C**) Schematic diagram of the synthesis of CREKA-Lipo-T nanoparticles.

Platelet inhibition prevented tumor cells from transitioning into invasive mesenchymal-like cells

In the primary tumor microenvironment, tumor-associated platelets secrete a relatively high level of TGF-β [5-6]. Increasing evidence shows that platelet-derived TGF-β plays a vital role in tumor cell transition into an invasive phenotype, the well-known epithelial-mesenchymal transition (EMT), and this in turn is an important step for tumor metastasis [5]. To determine whether ticagrelor could reduce the release of TGF-β from platelets, we first showed that incubating purified platelets with conditioned medium from 4T1 cells would stimulate TGF-β secretion (Figure S3). The amount of TGF-β secreted
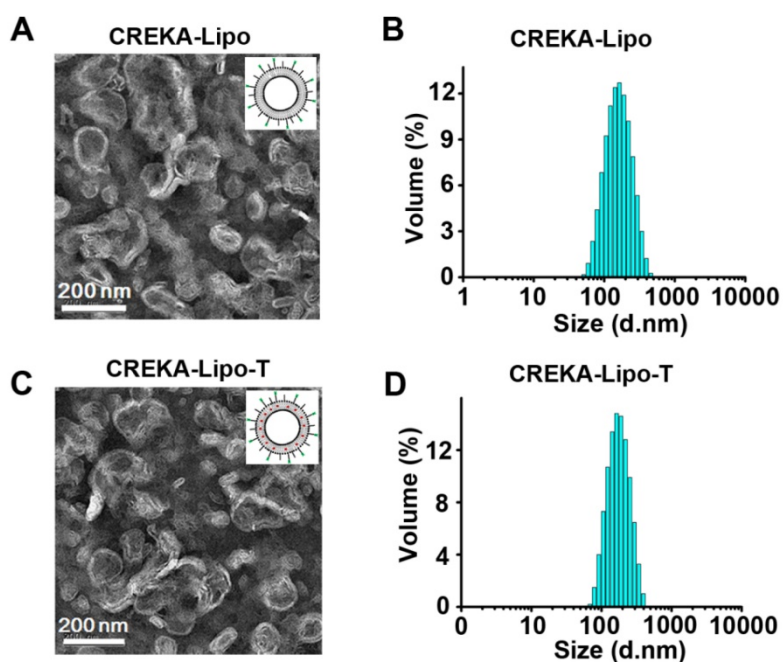
Figure 2. **Characterization of the CREKA-Lipo-T and CREKA-Lipo nanoparticles.** (**A,C**) TEM images of the representative empty (**A**) and drug-loaded (**C**) liposome nanoparticles. (**B,D**) DLS data showing the narrow size distribution of the two types of nanoparticles. The mean hydrodynamic diameter of empty particles (**B**) is smaller than that of CREKA-Lipo-T (**D**).

in response to treatment with tumor cell conditioned medium was significantly reduced in the presence of CREKA-Lipo-T, while the cells exposed to the control CREKA-Lipo nanoparticles did not show this effect.

We next investigated whether the inhibition of platelet function induced by CREKA-Lipo-T could affect the ability of tumor cells to transition into mesenchymal-like cells in vitro (Figure 3). We co-cultured mouse 4T1 mammary tumor cells with platelets, with or without CREKA-Lipo-T, at 37°C for 24 h, and examined tumor cell morphology by light microscopy. Tumor cells co-cultured with platelets showed a spindle-shaped, fibroblast-like appearance, which is typical of mesenchymal cells (Figure 3A). However, treatment with CREKA-Lipo-T, but not CREKA-Lipo, reduced this phenotypic transition. That platelets could induce EMT was supported by the higher level of expression of Snail protein and lower expression of E-cadherin in 4T1 tumor cells cocultured with platelets (Figure S4). These alterations in E-cadherin and Snail are characteristic of aggressive tumor cells [24]. The tumor cells-EMT inducing effects of platelets could be prevented by treatment with CREKA-Lipo-T, but not by CREKA-Lipo (Figure S3). We also investigated the invasive ability of 4T1 tumor cells treated with CREKA-Lipo-T in the presence of washed platelets in a Transwell assay (Figure 3B, C). Platelets significantly enhanced the invasiveness of 4T1 cells and this effect was inhibited by CREKA-Lipo-T, but

not CREKA-Lipo. Free ticagrelor was also able to prevent the enhanced cellular invasion induced by platelets. Together, these results suggest that ticagrelor released from CREKA-Lipo-T effectively inhibited platelet functions and thus blocked the transition of the tumor cells to a more aggressive and invasive phenotype.

Ticagrelor inhibits platelet-tumor cell interactions

Circulating platelets are able to adhere to tumor cells [25]. It has been proposed that such adhesion protects the tumor cells from the action of NK cells, thereby promoting the spread of cells via the bloodstream and, by doing this, supports metastasis [7-8, 25]. When CREKA-Lipo-T targets to the tumor blood vessel, the free ticagrelor was released slowly. In view of these findings, we investigated whether released free ticagrelor was able to affect platelet-tumor cell interactions *in vitro*. 4T1 tumor cells were incubated with washed, fluorescently labeled platelets in the absence or presence of ticagrelor for 1 h. Confocal microscopy showed that platelets associated with tumor cells in the absence of ticagrelor, but not in its presence (Figure S5). As shown in Figure S5, stronger inhibition of tumor cell adhesion associated with high concentration of ticagrelor in both free and nanoformulations of ticagrelor. These data suggest that the tumor-associated platelets treated with CREKA-Lipo-T *in vivo* might lose their ability to adhere to circulating tumor cells, thereby possibly reducing the likelihood of metastasis.

Plasma kinetics and tissue biodistribution of CREKA-Lipo-T

To evaluate the behavior of CREKA-Lipo-T nanoparticles *in vivo*, cy5.5-labeled CREKA-Lipo-T was administered intravenously to BALB/c mice and the plasma fluorescence intensity was measured by fluorescent imaging as a function of NP circulation with time post-injection. In these studies, CREKA-Lipo-T had a half-life about 3 h, whereas the half-life of free Cy5.5 was less than one hour (Figure 4 A, B). These results are consistent with other studies showing that nanoparticle formulations of drugs have an extended half-life compared to the free cy5.5 [15-16]. On the basis of this significant increase in plasma half-life, these results suggest that, compared with free dye, CREKA-Lipo-T nanoparticles are likely

to preferentially accumulate in the solid tumors.

We next evaluated whether the nanoparticles could accumulate in solid tumors. BALB/c nude mice bearing 4T1 tumor xenografts were treated by intravenous administration of saline, cy5.5-labeled Lipo-T (non-targeted NP), or cy5.5-labeled CREKA-Lipo-T, and the tumors and major organs were removed after 24 h. Twenty four hours after administration of CREKA-Lipo-T, the tumors had a significant 4-fold increase in fluorescence intensity relative to non-targeted nanoparticles at the same dose (Figure 4C, D). Little or no fluorescence was observed at several non-tumor sites in the body, including the liver, lung and kidney, suggesting highly specific active targeting of CREKA-Lipo-T to tumors. No fluorescence was observed in the organs in the saline treated control group.

In vivo anti-metastatic activity of CREKA-Lipo-T

CREKA-Lipo-T nanoparticles were next evaluated for their anti-metastatic activity. A mammary tumor xenograft model was established by implanting 4T1 cells into the mammary fat pads of syngeneic BALB/c mice. Metastasis formation in the lung, a preferential site of metastasis for 4T1 tumors, was examined. Mice whose primary tumors had reached ~300 mm^3 were treated with saline, free ticagrelor, CREKA-Lipo or CREKA-Lipo-T every other day for 16 days. After eight injections, the mice were sacrificed. Metastatic foci on the surface of lungs were counted (Figure 5A). A mean of 40 metastatic foci per lung were observed for the saline-treated control group, 22 foci/lung in mice treated with free drug (p=0.004) foci/lung in the CREKA-Lipo-treated controls. In striking contrast, a mean of 11 metastatic foci per lung were observed in the CREKA-Lipo-T-treated mice. Clearly, CREKA-Lipo-T outperformed free drug in reducing tumor metastasis formation (p=0.041), and this correlated with a substantially lower (p=0.023) lung weight (Figure 5B). These observations were further confirmed by performing H&E staining (Figure 5C, upper row), and immunostaining for proliferating cell nuclear antigen, PCNA [26] (Figure 5C, lower row) on formalin fixed sections of the lungs.
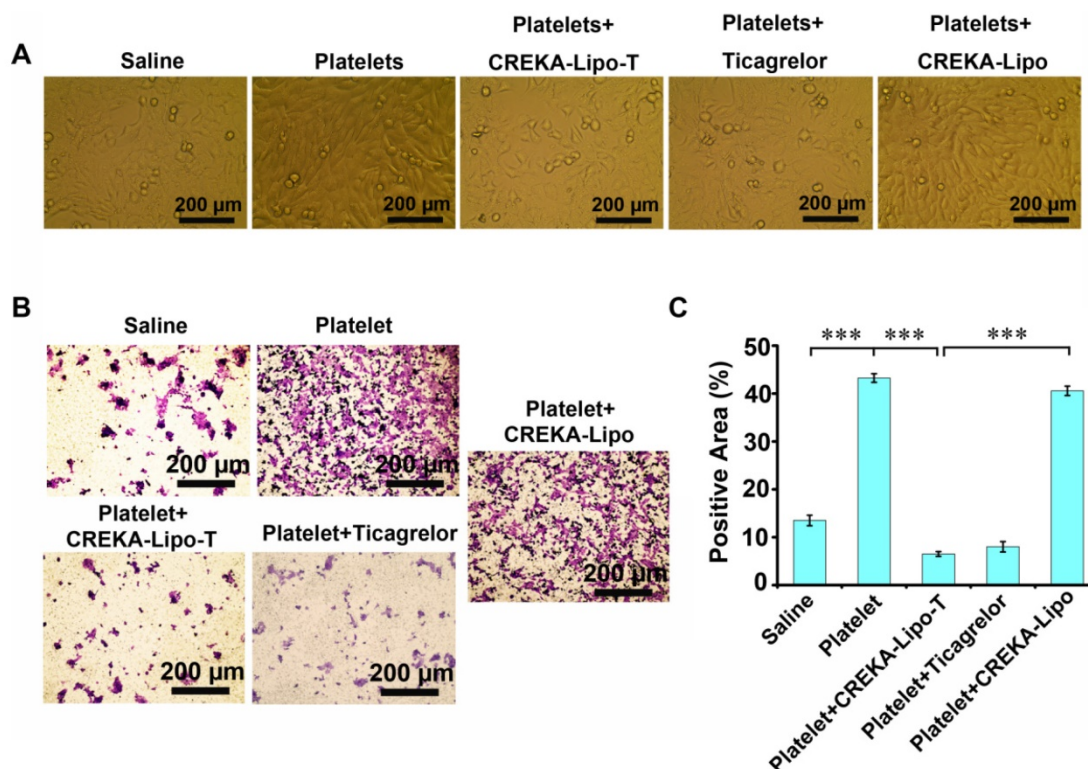
Figure 3. **CREKA-Lipo-T treatment blocks the transition of tumor cells to EMT-like invasive cells.** (**A**) The presence of CREKA-Lipo-T inhibited the platelet-induced invasive phenotype of 4T1 tumor cells as defined by the obvious morphological changes from polygonal to spindle-shaped cells. (**B**) Transwell migration assay of 4T1 tumor cells after treatment with platelets, platelets + ticagrelor, platelets + CREKA-Lipo-T, or platelets + CREKA-Lipo. (**C**) The data in B were quantified using image analysis software on the lower surface of the insert after crystal violet staining. Error bars represent the mean ± s.d. (n = 5); *** p<0.001.
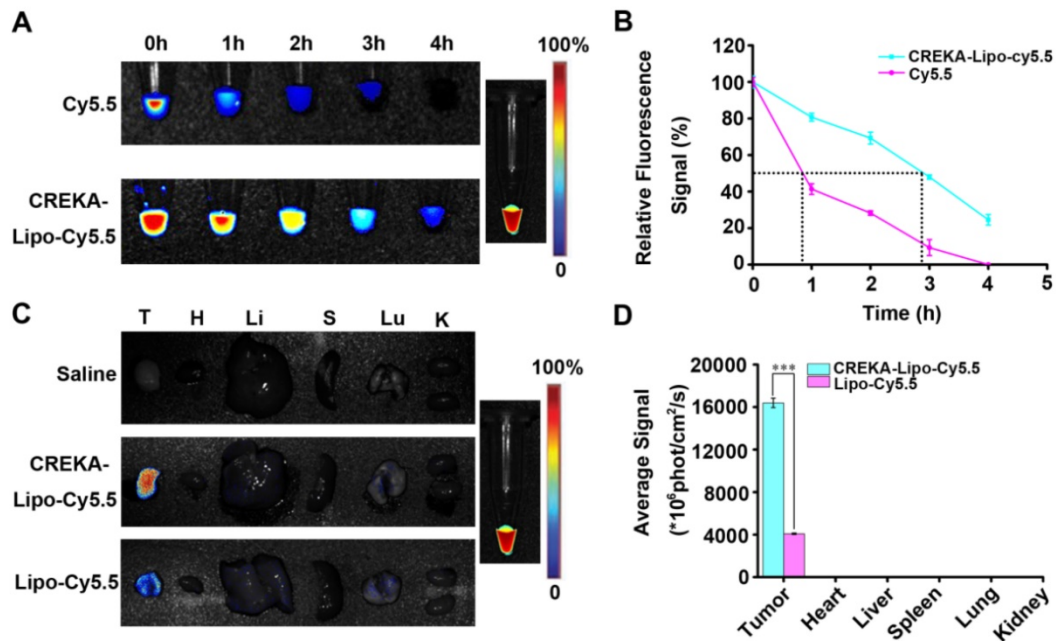
Figure 4. **Plasma clearance and *in vivo* tumor targeting of CREKA-Lipo-T.** (**A**) The plasma fluorescence signal was imaged at different times after intravenous injection of free cy5.5 (control) or cy5.5-CREKA-Lipo-T. (**B**) The plasma fluorescence intensity was quantified at several time points post-administration. The half-life was approximately 3 h for CREKA-Lipo-T and less than 1 h for free cy5.5. Error bars represent the mean ± s.d. of three independent experiments. (**C**) *Ex vivo* optical images of the tumors and other major organs from 4T1 tumor-bearing mice treated intravenously with saline, cy5.5-Lipo-T (without CREKA) or cy5.5-CREKA-Lipo-T for 24 h. A high-intensity fluorescent signal was detected only in the tumor region of mice injected with CREKA-Lipo-T. (**D**) The fluorescence intensities at the tumor sites and in normal organs were quantified 24 h post-injection. Error bars represent the mean ± s.d. of three independent experiments; *** $p<0.001$.
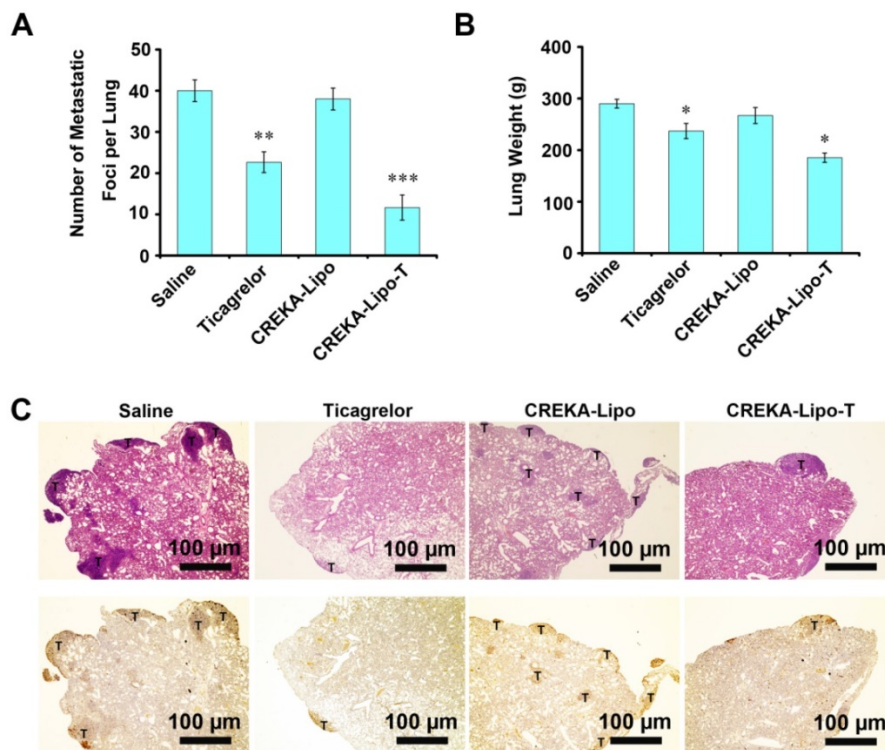
Figure 5. **Anti-metastatic activities of CREKA-Lipo-T *in vivo*.** (**A**) Quantification of metastatic foci. Error bars represent the mean ± s.d. (n = 5); **$p<0.01$; ***$p<0.001$. (**B**) Lung weights from animals in the treatment groups. Error bars represent the mean ± s.d; *$p<0.05$ *vs.* saline group. (**C**) H&E staining (upper row) and immunohistochemical staining for PCNA (lower row) for metastatic foci in the lungs of mice bearing 4T1 tumors after eight intravenous treatments (saline, ticagrelor alone, CREKA-Lipo or CREKA-Lipo-T) every two days for 16 days. T indicates metastases.
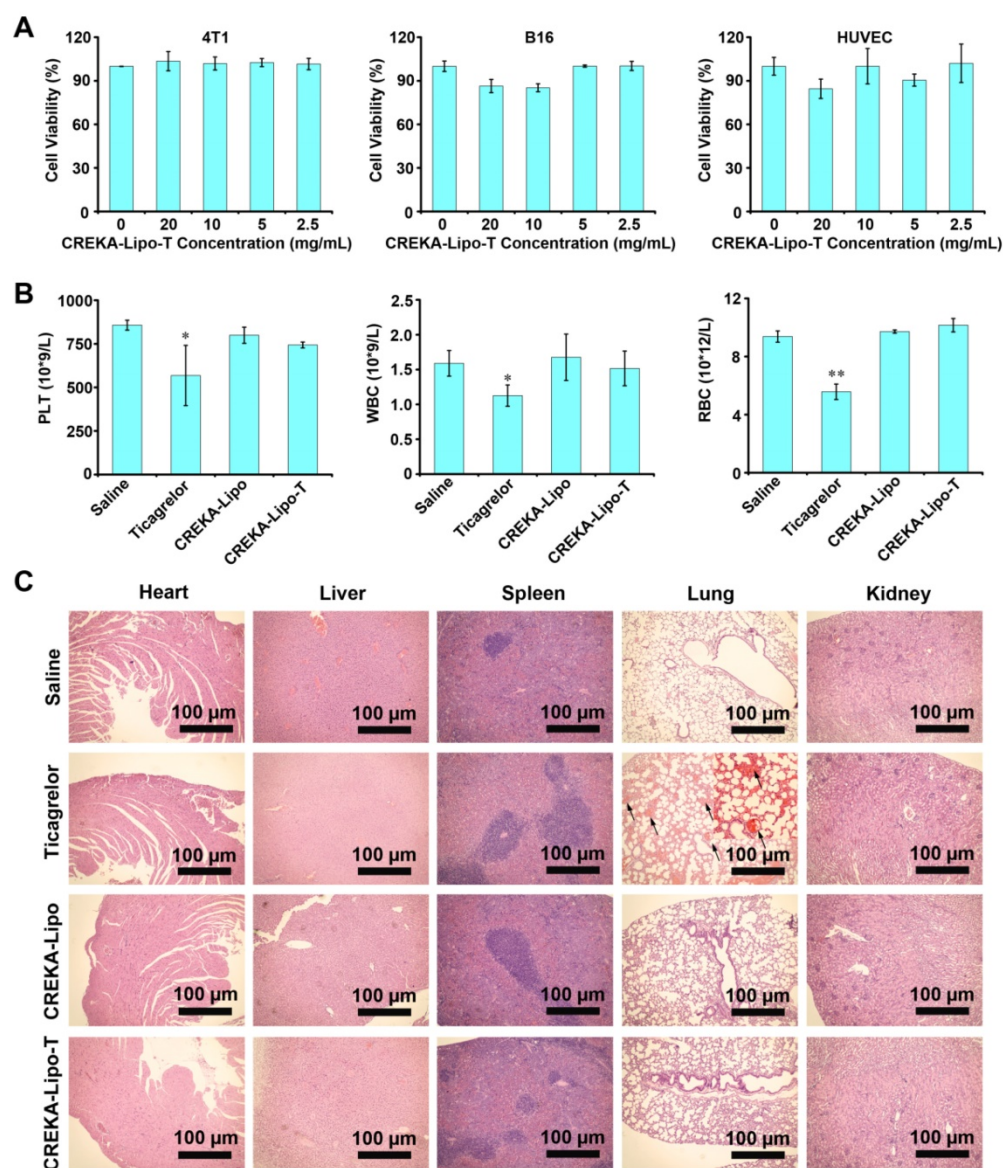
Figure 6. **Evaluation of the safety of CREKA-Lipo-T *in cultured cells* and *in vivo*.** (**A**) The effects of various doses of CREKA-Lipo-T on the viability of 4T1, B16 and HUVEC cell lines. Error bars represent the mean ± s.d. of three independent experiments. (**B**) Hematological analysis. The intravenous administration of CREKA-Lipo-T into mice on 8 consecutive occasions (every two days for 16 days) had no effect on circulating red cell, white cell or platelet counts, but free ticagrelor significantly reduced the numbers in each case. Error bars represent the mean ± s.d. of three independent experiments; *p<0.05. **p<0.01. (**C**) CREKA-Lipo-T treatment showed no visible damage to the major organs of mice as indicated by H&E staining. Black arrows indicate blood clots (n = 3). Insert is the enlarged area.

We examined the gross morphology of the lungs of treated mice and observed that treatment with CREKA-Lipo-T and ticagrelor alone led to fewer metastases compared to other control groups (Figure 5C & Figure S6). In addition, like other anti-platelet drugs, we found CREKA-Lipo-T had no effect on primary tumor volume (Figure S7). This observation supports the conclusion that CREKA-Lipo-T specifically inhibits the outgrowth of distant metastasis.

Safety of CREKA-Lipo-T nanoparticles

To investigate the potential side effects of CREKA-Lipo-T nanoparticles, we first investigated their cytotoxicity *in vitro* using three cell lines 4T1, B16-F10 and human umbilical vein endothelial cells (HUVEC) (Figure 6A). No obvious cytotoxicity was observed at concentrations of CREKA-Lipo-T nanoparticles up to 20 mg/mL. *In vivo*, no reduction in body weight was observed in any of the treatment groups in the tumor therapy experiments (Figure S8), and there were no significant differences in numbers of circulating red cells, white cells or platelets in female BALB/c mice following three successive injections (every other day) of CREKA-Lipo-T into the tail vein (Figure 6B). However, the cell and platelet numbers were dramatically reduced in the free ticagrelor-treated group (Figure 6B). Finally, we

examined the effects of CREKA-Lipo-T administration on histopathology of several major organs including the heart, liver, spleen, lung and kidney by H&E staining. As shown in Figure 6C, there were no obvious morphological changes or bleeding in the organs after CREKA-Lipo-T treatment. In contrast, free drug treatment resulted in extensive bleeding in the lungs (Figure 6C), which likely results from its systemic hematological toxicity, consistent with previous reports that that systemic administration of free platelet inhibitors leads to severe bleeding complications [14]. Since CREKA-Lipo-T could efficiently inhibit metastases without obvious bleeding and other side effects, this formulation has considerable potential for further preclinical development for the prevention of tumor metastases.

Conclusions

In this study, we describe a potential therapeutic approach for inhibiting tumor metastasis by specifically inhibiting tumor-associated platelet function with ticagrelor-loaded liposomal nanoparticles. The nanoparticles described have three important properties: (1) Specificity: the liposome nanocarriers incorporate effective active tumor homing peptides; (2) Simplicity: these self-assembling nanoparticles result from a simple two-step synthesis consisting of covalent peptide conjugation followed by typical liposome particle synthesis; and (3) Good tolerability: liposome nanoparticles have been used widely for drug delivery in the clinic and are biodegradable. These characteristics make the CREKA-Lipo-T formulation a particularly attractive therapeutic candidate for targeting of tumor metastasis.

Further work is needed to demonstrate the mechanisms underlying the anti-metastatic effect of our nanoplatform. Whether suppression of the platelet-secreted TGF-ß is the major factor in reduction of tumor metastases seen with CREKA-lipo-T needs to be studied in more detail. Our in vivo studies showed that CREK-Lipo-T has potent anti-metastatic effects in the highly aggressive 4T1 mouse mammary tumor model grown s.c in immune competent Balb/c mice. Dramatic reduction in number of metastasis was observed with the nanoformulation compared to control nanoparticles, and even to free drug, ticagrelor. These promising data need to be substantiated further in additional breast cancer models, such as the recently derived PDX models grown in the more relevant intraductal space, rather than s.c or in the mammary fat pad [27]. These studies will strengthen the observations made

in this paper and its potential for translation to the clinic.

Materials and methods

Materials

1,2-distearoyl-sn-glycero-3-phosphoethanolamine-N-[methoxy(polyethylene glycol)-2000] (DSPE-PEG-2000) and 1,2-distearoyl-sn-glycero-3-phosphoethanolamine-N-[maleimide (polyethylene glycol)-3400] (DSPE-PEG-3400-Mal) were purchased from Nuodepaisen Medical Technology Co. Ltd. (Suzhou, China). Ticagrelor was from Beijing Bailingwei Technology co., Ltd (Beijing, China). The peptide CREKA was synthesized by Taopu Biotechnology Co., Ltd (Shanghai, China). Cell counting kit-8 was purchased from Dojindo Molecular Technologies (Tokyo, Japan). TGF-β cytokine (R&D: 7666-MB-005), anti-E Cadherin antibody (Abcam: ab76055) and anti-SNAIL antibody (Abcam: ab53519) were obtained from Youningwei Biotechnology Co., Ltd (Shanghai, China).

Synthesis of DSPE-PEG-CREKA

DSPE-PEG-MAL (M_r 3800) (8.5 mg) and CREKA (M_r 647) peptide (1.78 mg) were dissolved in 4 mL 10% methanol purged with nitrogen and stirred for 4 h at room temperature. The solution was then dialyzed (molecular weight cutoff of M_r 1000) against double-distilled water for 24 h. The resulting DSPE-PEG-CREKA was lyophilized and stored for future use.

Preparation of CREKA-Lipo-T and CREKA-Lipo nanoparticles

Liposome nanoparticles were prepared by a filming-rehydration method. In brief, 17 mg lecithin, 2 mg DSPE-PEG, 1 mg DSPE-PEG-CREKA, 4 mg cholesterol and varying amounts of ticagrelor were dissolved in 10 mL dichloromethane in a round-bottom flask. After rotary evaporation for 40 min, a thin transparent film was formed. Tri-distilled water (10 mL) was then added and hydration was carried out for 20 min at 50°C. The final product was filtered using a 200 μm Liposome extruder. Free ticagrelor was removed by ultrafiltration (MWCO: 2000). The efficiency of encapsulation of ticagrelor into the liposome nanoparticles was calculated as follows: Encapsulation efficiency (%) = $W_t/W_0 \times 100\%$ (where W_0 and W_t are the amounts of initial ticagrelor and encapsulated ticagrelor respectively detected by UV-spectrophotometry at 270 nm). To normalize the nonspecific background of UV absorbance of the samples, we regarded the empty liposomes as the base line of adjustment.

Characterization of CREKA-Lipo-T and CREKA-Lipo

The size distribution, zeta potential and dispersity of CREKA-Lipo-T and CREKA-Lipo were evaluated by dynamic light scattering (DLS) using a ZetaSizer Nano series Nano-ZS (Malvern Instruments Ltd., Malvern, UK). The morphology of CREKA-Lipo-T and CREKA -Lipo were evaluated by transmission electron microscopy (TEM) (EM-200CX; JEOL Ltd., Tokyo, Japan) after negative staining with phosphotungstic acid solution on a carbon-coated copper grid. For assessing stability, the parameters described above for CREKA-Lipo-T and CREKA-Lipo were examined after storage of the nanoparticles for 10 days at 37 °C in PBS.

The drug release profiles of CREKA-Lipo-T

For measurement of the drug release profiles, CREKA-Lipo-T was maintained in dialysis bag (molecular weight cutoff of 1000 D), and placed in 30 mL PBS buffer, containing 2% Tween 80 in a 50 mL tube, general shaking at 37°C. At certain time intervals, 1 mL outside buffer was taken out for testing the amount of ticagrelor by UV-spectrophotometer at 270 nm. At the same time, 1 mL fresh PBS was added into the tube to maintain the consistent of total volume. The accumulative release of ticagrelor was calculated.

Cytotoxicity assay

The mouse breast cancer cell line 4T1 (American Type Culture Collection, ATCC, Manassas, VA, USA), mouse melanoma cell line B16 (ATCC) and human umbilical vein endothelial cells (HUVEC, ATCC) were maintained in 96-well plates at 37°C and subcultured for 24 h in RPM I 1640 (4T1,B16) or DMEM (HUVEC) with 10% fetal bovine serum (FBS) and 1% penicillin/streptomycin. Then the medium was replaced with fresh medium containing different concentrations of CREKA-Lipo-T. After a further 24 h, cell viability was assessed using a CCK-8 Kit. Five replicates were used in each case. The identity of the cell lines was confirmed by short tandem repeat DNA profiling followed by comparison with a standard database. All cell lines were tested regularly to ensure they were free from mycoplasma contamination.

Platelet preparation

Whole blood was drawn from BALB/c mice from the retro-orbital venous plexus and collected into anticoagulant (85 mM sodium citrate, 70 mM citric acid, 111 mM dextrose, pH 4.5) at a 1:9 ratio. Tyrode's buffer (138 mM NaCl, 2.9 mM KCl, 12 mM NaHCO$_3$, 0.36 mM NaH$_2$PO$_4$, 5.5 mM glucose, 1 mM CaCl$_2$ and 1 mM MgCl$_2$, 0.2% BSA, pH 7.4)(0.5 mL)

was then added and the tube was centrifuged at 180 g for 10 min at 4°C. The platelet-rich upper plasma layer was further centrifuged for 10 min at 850 g to collect the platelets. The platelets were resuspended in 1 mL of Tyrode's buffer for further use, then quantified by flow cytometry.

Western blot assay

The total proteins from culture medium were harvested from 4T1 mouse breast cancer cells after different treatments and analyzed by Western blot, with BSA as a loading control.

Confocal microscopy

4T1 breast cancer cells (1×10^5) were seeded onto 35 mm borosilicate coverslips and grown for 24 h. The medium was then replaced with fresh medium containing 2×10^6 fluorescently-labeled platelets (Dil stained for 20 min in Tyrode's buffer) and ticagrelor (0.1 mg/mL, 0.5 mg/mL), CREKA-Lipo-T(1 mg/mL, 5 mg/mL). As a control group, fresh medium containing platelets alone was added to coverslips covered by 4T1 tumor cells. After incubation for 1h, the cells were washed three times with PBS and the nuclei were stained with Hoechst 33342 for 3 min. The tumor cells were observed with an LSM 710 confocal microscope (Carl Zeiss, USA) at 63 × magnification.

The stability of nanoparticles *in vivo*

To investigate the half-life of nanoparticles, 100 μL cy 5.5 encapsulated CREKA-Lipo-T and 100 μL free cy5.5 were injected into the tail vein of Balb/C mice. At various time points after administration of the CREKA-Lipo-T and free cy5.5, 20 μL blood was withdrawn from a tail cut and subjected to fluorescent imaging using a CRi fluorescent imaging system.

In vivo biodistribution studies

Twenty four hours after the administration of 100 μL CREKA-Lipo-T-cy5.5 and 100 μL Lipo-T-cy5.5 (equivalent amounts of cy5.5), to BALB/c nude mice with 4T1 tumor xenografts, the animals were sacrificed and the tumor, heart, liver, spleen, lung, and kidneys were collected from each mouse for imaging using a CRi fluorescent imaging system.

Transwell cell invasion assay

The invasive ability of 4T1 cells was evaluated in a Transwell assay using Matrigel-coated filters (8μm pore size, BD, USA) in a 24-well plate. 4T1 cells at 5 × 104 were seeded into the upper chambers in FBS-free RPMI 1640 medium, then treated with PBS, platelets, platelets and CREKA-Lipo-T, ticagrelor, or platelets

and CREKA-Lipo（platelets: 2 × 106 Ticagrelor: 1mg/mL）, while the lower chambers contained RMPI 1640 medium with 10% FBS. After incubation for 24 h at 37°C with 5% CO_2, the lower surface of the insert was fixed with a 4% formaldehyde solution for 30 min and stained with 0.1% crystal violet for 20 min. The number of cells on the lower surface of the insert was quantified using image analysis software as an index of invasion.

Anti-metastasis effects *in vivo*

A tumor model was established in the BALB/c mouse by injecting mammary fat pads with 5 x 10^6 4T1 breast cancer cells per mouse (5 mice/group). When the tumor volume reached a size of ~300 mm³, various treatments (saline; ticagrelor; CREKA-Lipo; or CREKA-Lipo-T; the ticagrelor dose was 10 mg/kg in each case) were administered by tail vein injection every two days for 16 days. The size of tumors was measured using a vernier caliper on the day of treatment and 2, 6 and 15 days thereafter. The volume of the tumors was calculated using the formula: volume = [length × width²]/2. For the evaluation of metastasis, all the experimental mice were sacrificed on day 16 after 8 injections, and the primary tumor and lungs were collected, weighed and sectioned for histological analysis. Metastatic lung nodules were counted under the microscope by randomly selecting ten sections.

Statistical analysis

Statistical analysis was carried out by a Student's t-test or one-way ANOVA with SPSS 19.0 (SPSS Inc., Chicago, IL). Quantitative data are presented as mean ± s.d. Tumor volumes were compared using a Kruskal-Wallis test followed by the Mann-Whitney test. Two-sided P values less than 0.05 were considered statistically significant.

Supplementary Material

Supplementary figures and tables.
http://www.thno.org/v07p1062s1.pdf

Acknowledgments

Competing Interests

The authors have declared that no competing interest exists.

References

[1] Barker HE, Chang J, Cox TR, Lang G, Bird D, Nicolau M, et al. LOXL2-mediated matrix remodeling in metastasis and mammary gland involution. Cancer Res. 2011; 71:1561-72.

[2] Valastyan S, Weinberg RA. Tumor metastasis: molecular insights and evolving paradigms. Cell. 2011; 147:275-292.

[3] Quail DF, Joyce JA. Microenvironmental regulation of tumor progression and metastasis. Nat Med. 2013; 19:1423-37.

[4] Gay LJ, Felding-Habermann B. Contribution of platelets to tumour metastasis. Nat Rev Cancer. 2011; 11:123-34.

[5] Labelle M, Begum S, Hynes RO. Direct signaling between platelets and cancer cells induces an epithelial-mesenchymal-like transition and promotes metastasis. Cancer Cell. 2011; 20:576-90.

[6] Ge R, Rajeev V, Ray P, Lattime E, Rittling S, Medicherla S, et al. Inhibition of growth and metastasis of mouse mammary carcinoma by selective inhibitor of transforming growth factor-β type I receptor kinase in vivo. Clin Cancer Res. 2006; 12:4315-30.

[7] Nieswandt B, Hafner M, Echtenacher B, Männel DN. Lysis of tumor cells by natural killer cells in mice is impeded by platelets. Cancer Res. 1999; 59:1295-300.

[8] Placke T, Örgel M, Schaller M, Jung G, Rammensee H-G, Kopp H-G, et al. Platelet-derived MHC class I confers a pseudonormal phenotype to cancer cells that subverts the antitumor reactivity of natural killer immune cells. Cancer Res. 2012; 72:440-8.

[9] Schumacher D, Strilic B, Sivaraj KK, Wettschureck N, Offermanns S. Platelet-derived nucleotides promote tumor-cell transendothelial migration and metastasis via P2Y 2 receptor. Cancer Cell. 2013; 24:130-7.

[10] Sierko E, Wojtukiewicz MZ. Inhibition of platelet function: does it offer a chance of better cancer progression control?. Semin Thromb Hemost. 2007; 33:712-21.

[11] Wang Y, Sun Y, Li D, Zhang L, Wang K, Zuo Y. et al. Platelet P2Y12 is involved in murine pulmonary metastasis. PloS one. 2013; 8:e80780.

[12] Cooke NM, Spillane CD, Sheils O, O'Leary J, Kenny D. Aspirin and P2Y 12 inhibition attenuate platelet-induced ovarian cancer cell invasion. BMC Cancer. 2015; 15:627.

[13] Gebremeskel S, LeVatte T, Liwski RS, Johnston B, Bezuhly M. The reversible P2Y12 inhibitor ticagrelor inhibits metastasis and improves survival in mouse models of cancer. Int J Cancer. 2015; 136:234-40.

[14] Tesfamariam B. Involvement of platelets in tumor cell metastasis. Pharmacol Ther. 2016; 157:112-119.

[15] Wang H, Wu Y, Zhao R, Nie G. Engineering the assemblies of biomaterial nanocarriers for delivery of multiple theranostic agents with enhanced antitumor efficacy. Adv Mater. 2013; 25:1616-22.

[16] Li F, Zhao X, Wang H, Zhao R, Ji T, Ren H, et al. Multiple layer-by-layer lipid-polymer hybrid nanoparticles for improved FOLFIRINOX chemotherapy in pancreatic tumor models. Adv Funct Mater. 2015; 25:788-98.

[17] Devulapally R, Sekar NM, Sekar TV, Foygel K, Massoud TF, Willmann JrK, et al. Polymer nanoparticles mediated codelivery of antimiR-10b and antimiR-21 for achieving triple negative breast cancer therapy. ACS Nano. 2015; 9:2290-302.

[18] Bozzuto G, Molinari A. Liposomes as nanomedical devices. Int J Nanomedicine. 2015; 10:975-999.

[19] Schömig A. Ticagrelor–is there need for a new player in the antiplatelet-therapy field. N Engl J Med. 2009; 361:1108-11.

[20] Simberg D, Duza T, Park JH, Essler M, Pilch J, Zhang L, et al. Biomimetic amplification of nanoparticle homing to tumors. Proc Natl Acad Sci U S A. 2007; 104:932-6.

[21] Peters D, Kastantin M, Kotamraju VR, Karmali PP, Gujraty K, Tirrell M, et al. Targeting atherosclerosis by using modular, multifunctional micelles. Proc Natl Acad Sci U S A. 2009; 106:9815-9.

[22] Qin C, Fei J, Wang A, Yang Y, Li J. Rational assembly of a biointerfaced core@ shell nanocomplex towards selective and highly efficient synergistic photothermal/photodynamic therapy. Nanoscale. 2015; 7:20197-20210.

[23] Miyako E, Kono K, Yuba E, Hosokawa C, Nagai H, Hagihara Y. Carbon nanotube–liposome supramolecular nanotrains for intelligent molecular-transport systems. Nat Commun. 2012; 3:1226.

[24] Huber M A, Kraut N, Beug H. Molecular requirements for epithelial–mesenchymal transition during tumor progression. Curr Opin Cell Biol. 2005; 17:548-558.

[25] Palumbo JS, Talmage KE, Massari JV, La Jeunesse CM, Flick MJ, Kombrinck KW, et al. Platelets and fibrin (ogen) increase metastatic potential by impeding natural killer cell–mediated elimination of tumor cells. Blood. 2005; 105:178-185.

[26] Mahler M, Miyachi K, Peebles C, Fritzler MJ. The clinical significance of autoantibodies to the proliferating cell nuclear antigen (PCNA). Autoimmun Rev. 2012; 11:771-775.

[27] Sflomos G, Dormoy V, Metsalu T, Jeitziner R, Battista L, Scabia V, Vilo J, et al. A Preclinical Model for ERα-Positive Breast Cancer Points to the Epithelial Microenvironment as Determinant of Luminal Phenotype and Hormone Response. Cancer cell. 2016; 29:407-422.